Preliminary design and simulation of a 162.5 MHz high-intensity proton RFQ for an accelerator driven system*

XIAO Chen(肖陈)[1,2;1)] HE Yuan(何源)[1] LIU Yong(刘勇)[1] YUAN You-Jin(原有进)[1]
WANG Zhi-Jun(王志军)[1,2,3] HE Shou-Bo(贺守波)[1,2] XU Meng-Xin(徐孟鑫)[1,2]
LI Chao(李超)[1,2] YUE Wei-Ming(岳伟明)[1] CHANG Wei(常玮)[1,2]
ZHAO Hong-Wei(赵红卫)[1] XIA Jia-Wen(夏佳文)[1]

[1] Institute of Modern Physics, Chinese Academy of Sciences, Lanzhou 730000, China
[2] Graduate University of Chinese Academy of Sciences, Beijing 100049, China
[3] School of Nuclear Science and Technology, Lanzhou University, Lanzhou 730000, China

Abstract: A new procedure for the design and simulation of a Radio Frequency Quadrupole (RFQ) accelerator has been developed at the Argonne National Laboratory. This procedure is integrated with the beam dynamics design code DESRFQ and the simulation code TRACK, which are based on three-dimensional field calculations and the particle-in-cell mode beam dynamics simulations. This procedure has been applied to the development of a 162.5 MHz CW RFQ which is capable of delivering a 10 mA proton beam for the Accelerator Driven System (ADS) of the CAS. The simulation results show that this RFQ structure is characterized by the stable values of the beam acceleration efficiency for both the zero current beam and space charge dominated beam. For an average beam current of 10 mA, there is no transverse rms emittance growth, the longitudinal rms emittance at the exit of RFQ is low enough and there is no halo formation. The beam accelerated in the RFQ could be accepted easily and smoothly by the following super-conducting linear accelerator.

Key words: RFQ, DESRFQ, TRACK, ADS, space charge effect

PACS: 29.27.Bd, 52.65.Rr, 41.20.cv **DOI:** 10.1088/1674-1137/35/11/014

1 Introduction

Nuclear power as a clean energy source would be a good choice and play an increasingly important role in adjusting the existing energy structure in China for the sustainable development of the national economy. The ADS is a new device for clean energy and now this technology is under study in the CAS for the

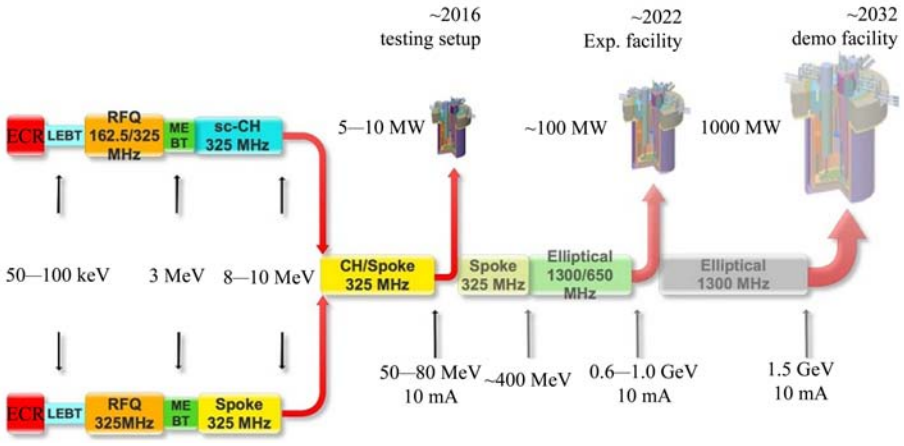

Fig. 1. (color online) The conceptual design of the ADS project.

Received 19 January 2011
* Supported by National Natural Science Foundation of China (10635090)
1) E-mail: xiaochen@impcas.ac.cn

purpose of providing a new option for the development of nuclear power stations. Fig. 1 depicts the conceptual design of the ADS project of the CAS which is divided into three stages.

A 162.5 MHz RFQ has been designed to serve as an initial accelerator structure for the ADS. The design of the RFQ has been iterated several times to satisfy more advanced RFQ beam specifications. In particular, the longitudinal phase space beam emittance must be halo free and low enough to avoid excessive beam loss in the following high energy section.

2 RFQ structure design

For the beam dynamics design, the RFQ is divided into three main sections: an input radial matcher, a main modulated vane section where bunching and acceleration occur, and an output radial matcher.

The structures of the input radial matching section and the main section of the RFQ are generated by the DESRFQ code [1]. This code uses a Laplace equation solver, which takes into account the physical vane shape to generate the RFQ vane tip geometry in every cell and the RFQ parameters required for the final simulation via the TRACK code [2]. Fig. 2 shows the beam dynamics simulation of this RFQ via the DESRFQ code in the transverse and the longitudinal phase planes.

The DESRFQ code gives users the flexibility to alter the synchronous phase and modulation at any given cell, and users could see the result graphically on the separatrix. Table 1 lists the main basic parameters which are generated by the DESRFQ code.

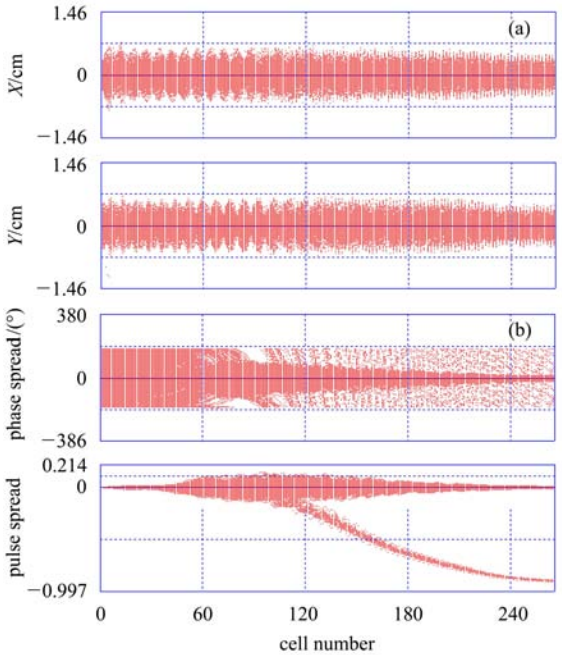

Fig. 2. (a) The multi-particle trajectories in the transverse planes. (b) The multi-particle trajectories in the longitudinal planes.

Table 1. Initial specifications for the RFQ design.

parameter	value
operation frequency	162.5 MHz
beam current	10 mA
average radius	0.75 cm
vane voltage	115.79 kV
vane curvature radius	0.6 cm
input energy	40 keV
output energy	3 MeV
vane length	617.12 cm
kilpatrick unit	1.4

Figure 3 illustrates some oscillations of the beam parameters as a function of the cell number. An average beam current of 20 mA is considered in the RFQ design for the space charge effect calculations.

This RFQ structure has been extensively calculated employing the DESRFQ code to reach an optimum compromise between the following four conflicting requirements: (1) to form low longitudinal emittance output; (2) to avoid transverse rms emittance growth; (3) to maximize beam transmission; and (4) to maximize the accelerating rate. Conditions (1) and (2) could be satisfied at a relatively low amplitude of the initial accelerating field (small modulation coefficient at the initial bunching section), and increase the modulation coefficient slowly. While conditions (3) and (4) require a high modulation coefficient at the initial bunching section and increase the modulation coefficient rapidly. After the optimization, the final RFQ modulation and synchronous phase as a function of the cell number are given in Picture (a).

In the smooth approximation the transverse phase advance is given by the following expressions:

$$\mu^2 = \frac{2}{\pi^2}K^4 + 2\gamma_0 \sin\varphi_{\rm s}, \tag{1}$$

$$K^2 = \left(\frac{\lambda}{2R_0}\right)^2 \frac{ZU_{\rm L}}{A\varepsilon_0}, \quad \gamma_0 = \pi^2 \frac{ZU_{\rm L}T}{A\pi\beta^2\varepsilon_0}, \tag{2}$$

$$T = \frac{\pi}{4}\frac{m^2-1}{m^2 I_0\left(\frac{2\pi}{\beta\lambda}\cdot\frac{2R_0}{m+1}\right) + I_0\left(m\cdot\frac{2\pi}{\beta\lambda}\cdot\frac{2R_0}{m+1}\right)}, \tag{3}$$

here the parameter K represents the rigidity of the focusing channel and does not depend on the particle phase, γ_0 is the defocusing factor, $\varphi_{\rm s}$ is the synchron-

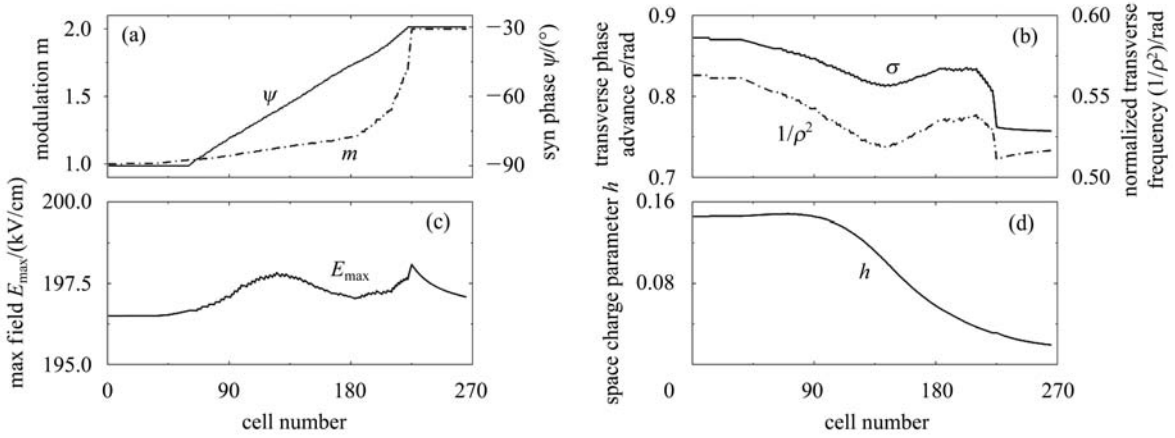

Fig. 3. (a) The modulation coefficient and synchronous phase. (b) The transverse phase advance and normalized transverse frequency. (c) The peak surface field. (d) The space charge parameter.

ous phase, λ is the wave length, R_0 is the average radius, Z is the charge number, A is the mass number, $U_{\rm L}$ is the vane voltage, ε_0 is the rest mass, T is the acceleration efficiency, β is the particle velocity, and m is the modulation. Another important relation between the rate of floquet phase change and the square of the floquet modulus is given as:

$$\frac{{\rm d}\Phi}{{\rm d}\tau}=\frac{1}{\rho^2}\,,\quad R_{\rm env}(0)=\rho\sqrt{\frac{S}{\beta\gamma}\varepsilon_{\rm n}}, \tag{4}$$

here $\varepsilon_{\rm n}$ is the transverse normalized beam emittance and S is the focusing period length. The rate of floquet phase change is inversely proportional to the square of beam envelope for zero current. Accumulation of particles close to the lower transverse phase advance is a sign of halo formation in the transverse phase space. It is seen from Picture (b) that the lowest transverse phase advance at the end of the RFQ is still far from the unstable area.

Peak surface field $E_{\rm max}$ is the most important initial parameter of the RFQ design. The choice of the peak surface could be based on broad operational experiences. Using the kilpatrick limit is a common way of evaluating the peak tolerable surface field in the RFQ. However, there are discrepancies in the definition of the kilpatrick limit in the literature. In many cases the kilpatrick limit is calculated without taking into account the gap between the electrodes [3]. The following expressions are used in the DESRFQ code:

$$E_{\rm max}=\chi\frac{U_{\rm L}}{R_0}, \tag{5}$$

$$\chi=\sqrt{\frac{1}{2}\left(1+\frac{R_{\rm e}}{R_0}\right)^2+\frac{2T}{\pi}\frac{2\pi}{\beta\lambda}R_0I_0\left(\frac{2\pi}{\beta\lambda}\frac{R_0+R_{\rm e}}{\sqrt{2}}\right)^2}, \tag{6}$$

here $R_{\rm e}$ is the vane curvature radius. The only way to decrease χ at the given R_0 is to decrease $R_{\rm e}$. However, decreasing $R_{\rm e}$ means increasing the high order field, which is not good for beam acceleration efficiency. In Picture (c), the maximum value of the electric field is below 200 kV/cm and this RFQ accelerator could be operated at the CW mode in safety.

The space charge effect on the transverse motion is described by a parameter h which is introduced as:

$$h=\frac{\lambda}{\mu(0)I_0}\frac{IB_{\rm f}}{\beta\gamma^2\varepsilon_{\rm n}}, \tag{7}$$

here I is the beam average current, $B_{\rm f}$ is the bunching factor, $\mu(0)$ is the phase advance of the transverse oscillations for zero current, and I_0 is the characteristic current defined by the expression:

$$I_0=4\pi\varepsilon_0\frac{Am_0c^3}{qZ}, \tag{8}$$

here the characteristic beam current is I_0=3.17×10^7 A for protons. The matched beam envelopes in the presence of the space charge effect must be increased according to Eq. (9) and the transverse phase advance is shown as Eq. (10):

$$R_{\rm env}(h)=R\sqrt{h+\sqrt{1+h^2}},\quad \mu(h)=\mu(\sqrt{1+h^2}-h). \tag{9}$$

According to Exp. (7), to keep the space charge parameter constant along the low energy section and to avoid an excessive space charge effect, the bunching factor should be proportional to the beam velocity in this section. In the process of simulation, the space charge parameter reaches its maximum value $h_{\rm max}$=0.1482 at the end of the pre-buncher section. It results in a 7.7% envelope size increase and a 13.7% transverse phase advance decrease.

3 Beam dynamics simulation

3.1 Transverse beam dynamics simulation

The multi-particle dynamics simulations of this RFQ have been performed using the TRACK code. This code tracks the particles through the whole RFQ in both the three-dimensional external electric field and the internal space charge field. The three-dimensional electric field in the regular section is expressed by an 8-term Fourier-Bessel expansion. These terms are the same as those in the PARMTEQ-M code [4]. The particle motion in the realistic field is nonlinear and the most comprehensive beam dynamics studies could be carried out by numerical simulations. The beam dynamics simulations of the three different beam currents are shown in Fig. 4.

The beam dynamics simulations are performed with a beam represented as a collection of 10,000 macro-particles. The beam rms size at 20 mA reaches its maximum value at the end of the pre-buncher section as predicted by expression (9).

In the low energy section, the velocity of the particle is low and the space charge effect is strong and the beam envelope's growth along the bunching section reflects some beam halo formations. Further envelope growth is limited by the aperture and particle losses. Despite some halo formation, the total particle losses do not exceed 7% and most particles are lost in the cells with the large space charge parameter.

The transverse normalized emittance in the horizontal and vertical directions at the exit of the RFQ and the acceleration efficiencies of several injection situations are shown in Table 2. The unit of the transverse normalized emittance is π·cm·mrad.

The simulation results illustrate that a further increase of the beam current results in a larger number of particles approaching the non-stability border, and leads to a higher emittance growth. This trend is clearly observed in Table 2.

The proposed design of this RFQ is capable of efficiently accelerating high-current beams. The value of the limited beam current of this RFQ could be estimated to be round 45 mA. The simulations have been carried out assuming the input emittance is a constant independent of the input beam current. The higher beam current means larger matched beam envelopes at the main section of the RFQ, and a more convergent angle for injection at the input radial matching section. The matched injection Twiss parameters and the mismatched factors of the several beam currents are demonstrated in Table 3.

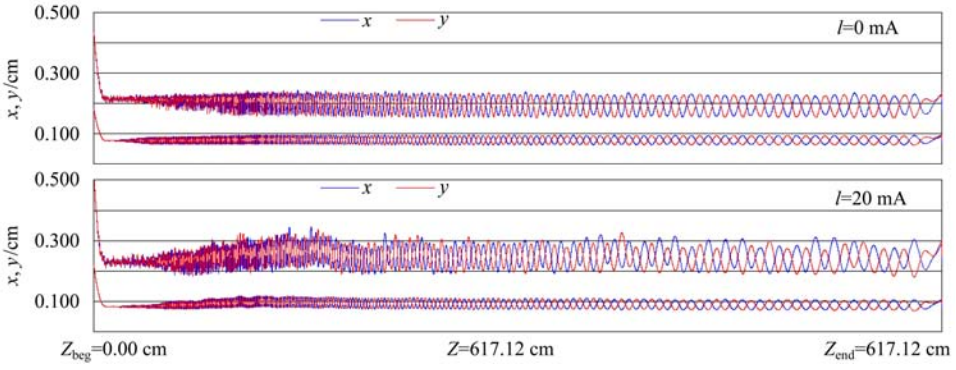

Fig. 4. (color online) The beam envelopes along the RFQ when the average beam current is chosen to be 0 mA, 20 mA. The pairs of the lower curves are the beam rms sizes, and the upper curves are the beam envelopes.

Table 2. The transverse normalized emittance and the acceleration efficiency of the different injection currents.

current	ε_{nx}(4rms)	ε_{nx}(99.5%)	ε_{nx}(100%)	ε_{ny}(4rms)	ε_{ny}(99.5%)	ε_{ny}(100%)	efficiency (%)
input	0.10038	0.14065	0.14978	0.10000	0.14053	0.14903	
0 mA	0.10056	0.14165	0.16509	0.09972	0.14154	0.15814	98.66
5 mA	0.10131	0.17535	0.25636	0.10000	0.16732	0.25313	97.85
10 mA	0.10022	0.16092	0.24308	0.10026	0.16064	0.24303	97.23
15 mA	0.10073	0.16020	0.21023	0.09993	0.15858	0.20729	95.95
20 mA	0.10232	0.16124	0.25675	0.10080	0.16407	0.21419	92.81

Table 3. The matched injection Twiss parameters and the mismatched factors for the different beam currents.

current/mA	α	β/(cm/rad)	mismatch
0	1.52908	12.13	1.02664
5	1.77863	13.45	1.02940
10	2.04202	14.83	1.03245
15	2.31797	16.27	1.03697
20	2.60525	17.76	1.04049

When the value of the input beam current is chosen to be 20 mA, the horizontal and vertical beam nature emittance and the intensity distributions at the exit of the RFQ are shown in Fig. 5.

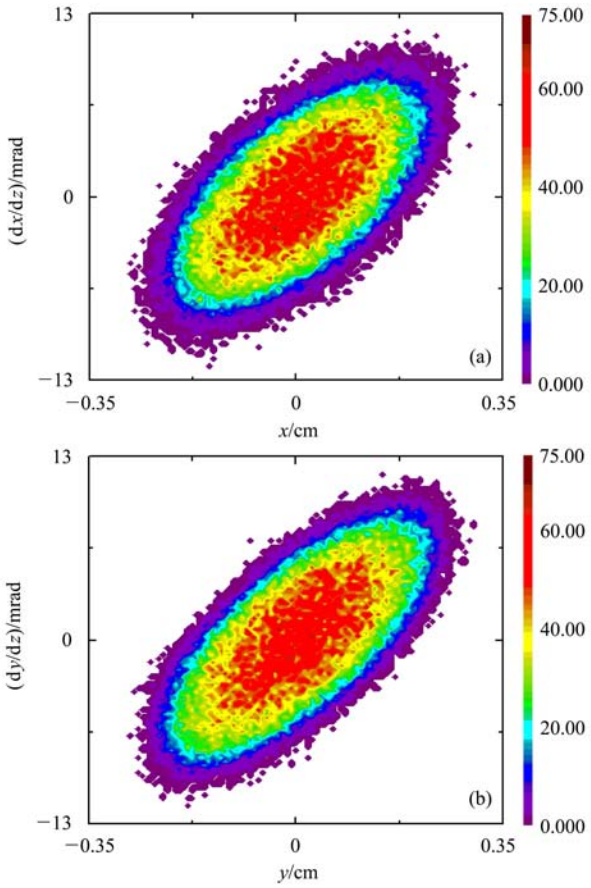

Fig. 5. The horizontal and vertical beam emittances at the exit of the RFQ.

According to particle distributions analysis, there is no beam halo formation, the beam rms emittance growth is not obvious and the particle distribution is essentially Gaussian.

3.2 Longitudinal beam dynamics simulation

The values of four times the rms, the 99.5% of particles and the total longitudinal emittance are listed correspondingly in Table 4, and the unit of longitudinal emittance is keV/u·deg.

Table 4. The longitudinal emittance at the exit of the RFQ of different injection currents.

current/mA	ε_{nz}(4rms)	ε_{nz}(99.5%)	ε_{nz}(100%)
0	370.229	948.313	1185.391
5	229.203	976.875	1667.021
10	231.843	887.700	1713.841
15	245.805	1542.959	2051.807
20	251.936	937.888	2058.961

After optimization, four times the rms longitudinal emittance would reach the smallest value at about 10 mA (the operated beam current). The total longitudinal emittance is always proportional to the beam current. The profile and intensity of the longitudinal emittance at the exit of the RFQ for zero beam current and 20 mA beam current are illustrated in Fig. 6.

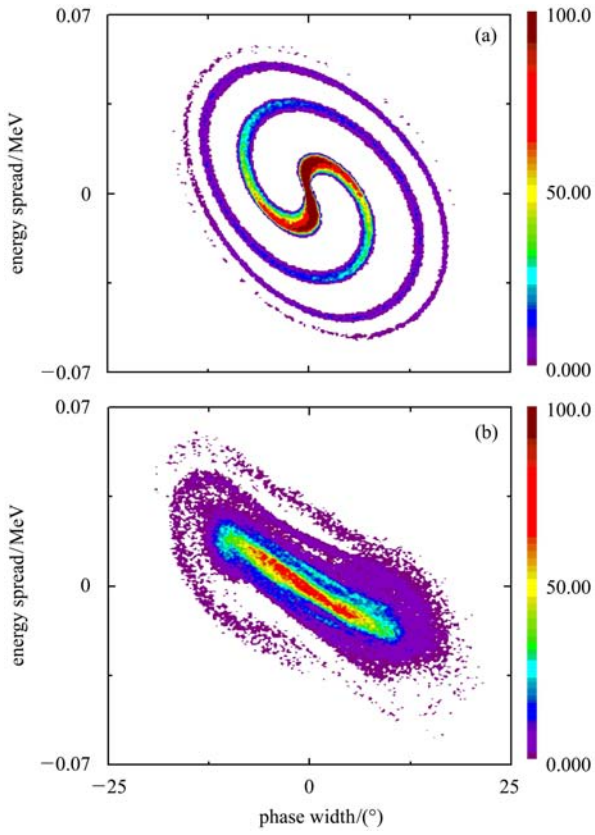

Fig. 6. The longitudinal beam emittance at the exit of the RFQ of 0 mA and 20 mA beam currents.

Picture (a) is the particle distribution in the longitudinal phase space for the zero current beam. Most particles are concentrated in the center of the core, only a small number of particles are outside the core and are distributed in the tail area.

Picture (b) is the particle distribution of the 20 mA beam. The particles are still compact in the beam

core, but become sparser farther from the core due to the strong space charge effect.

3.3 Beam dynamics simulations for the 2-term or the 8-term Fourier-Bessel field expansion

In the regular accelerating cells, the electric field is calculated using either the first 2-term or the total 8-term Fourier-Bessel field expansion. Expansion coefficients have been obtained from the DESRFQ code as described above.

The beam dynamics simulations for the 2-term and 8-term expansions are given for comparison in Table 5. Simulation with the 8-term potential expansion shows slightly higher beam losses and higher beam emittance growths in the main part of the RFQ.

Table 5. The simulation results when the beam current is 20 mA for 2-term or 8-term potential expansions, respectively.

parameter	2-term	8-term
output energy/MeV	3.02549	3.02536
ε_{nx}(4rms)/(π·cm·mrad)	0.10152	0.10232
ε_{ny}(4rms)/(π·cm·mrad)	0.10165	0.10080
ε_{nz}(4rms)/(keV/u·deg)	249.265	251.936
ε_{nz}(99.5%)/(keV/u·deg)	965.039	973.888
T-efficiency (%)	99.78	99.10
A-efficiency (%)	92.76	92.81

4 Conclusion

A new procedure has been developed for designing the structure of the high-intensity RFQ. This procedure is a modification of the previously well-known RFQ design concepts unified with the new entirely three-dimensional field calculations for the design and simulation of the RFQ.

The influences of the space charge effect are calculated in detail, the transmission efficiency and the acceleration efficiency, the input matched Twiss parameters and the transverse emittance at the exit of the RFQ are extremely sensitive to the injection beam currents.

When the beam current is lower than 20 mA, the longitudinal rms emittance is relatively low. For the designed beam current (10 mA average beam current), there is no transverse rms emittance growth (lower than 1%). The longitudinal rms emittance is relatively low and there is no beam halo formation. Most particles accelerated in the RFQ could be accepted smoothly by the following super-conducting linear accelerator.

One of the authors, Xiao Chen, would like to express his sincere thanks to Andrei Kolomiets and Brahim Mustapha at the Argonne National Laboratory for their valuable suggestions and great help.

References

1 Kolomiets A A et al. The RFQ design software DesRFQ. ITEP/ ANL Technical Note, 2005
2 http://www.phy.anl.gov/atlas/TRACK/. TRACK code, a code for the beam dynamics simulation in accelerator and transport lines with 3D electric and magnetic field, by P.N.Ostroumov, V.N.Aseev and B.Mustapha
3 Kapchinsky I M. Theory of linear resonance accelerator. New York: 1982 (in Russian)
4 http://laacg1.lanl.gov/. PARMTEQ-M code, a code for RFQ design code, by K.R.Crandall, Wangler T P and Young L M